Atmospheric patterns driving Holocene productivity in the Alboran Sea (Western Mediterranean): a multiproxy approach

Blanca Ausín[1]; Jose A Flores[1]; Francisco J Sierro[1]; Isabel Cacho[2]; Iván Hernández-Almeida[3]; Belén Martrat[4]; Joan O Grimalt[4]

[1]Department of Geology, University of Salamanca. Pza/ de la Merced s/n, 37008 Salamanca, Spain.

[2]Department of Stratigraphy, Paleontology and Marine Geosciences, University of Barcelona, C/Martí i Franquès s/n, 08028 Barcelona, Spain.

[3]Institute of Geography and Oeschger Centre for Climate Change Research, University of Bern, Erlachstrasse 9a, CH-3012 Bern, Switzerland.

[4]Department of Environmental Chemistry. Institute of Environmental Assessment and Water Research, C/Jordi Girona 18, 08034 Barcelona, Spain.

Email: b_ausin@usal.es

Abstract

High-resolution paleoproductivity variations have been reconstructed in a productive cell in the Alboran Sea for the Holocene. Fossil coccolithophore assemblages have been studied along with the $U^{k'}_{37}$-estimated sea-surface temperature (SST) and other paleoenvironmental proxies. The appearance of this cell is suggested at 7.7 ka cal BP and was linked to the establishment of the western anticyclonic gyre. From that time until the present, the nannofossil accumulation rate of *Florisphaera profunda* has revealed successive episodes of weakening and strengthening of upwelling conditions in the Alboran Sea that have been simultaneous to changes in Western Mediterranean Deep Water (WMDW) formation in the Gulf of Lions. A two-phase scenario operating at millennial-centennial time-scale is proposed to explain this climatic and oceanographic variability: [1] coeval with more arid climate conditions, weaker northerlies/north-westerlies blowing over the Gulf of Lions would have triggered a slackening of WMDW

formation. This together with a minor Atlantic Jet (AJ) inflowing into the Alboran Sea would have led to less vertical mixing, and hence, a more stable water column in the study area; [2] wetter climate conditions would have prevailed in the region while stronger northerlies/north-westerlies would have enabled WMDW reinforcement in the Gulf of Lions simultaneous to an intensification of the AJ that migrated southward. This would have increased vertical mixing, intensifying upwelling conditions in the study area. Here, the winter North Atlantic Oscillation (NAO) is considered to be an important forcing mechanism for this variability, influencing WMDW formation, which in turn has been linked to short-term productivity variations during the last 7.7 kyr in the Alboran Sea.

Keywords

Coccolithophore productivity, Holocene, Western Mediterranean Deep Water, North Atlantic Oscillation, Alboran Sea

Introduction

In recent years, climatic variability during the Holocene (11.7 kyr to present) has been a challenging issue. Recent studies have shown that this period has been characterised by several abrupt climatic events as well as pervasive short-term oscillations (Mayewski et al., 2004; Wanner et al., 2011), ruling out the perception of the Holocene as having been stable. As the most recent geological period, the variability recorded by the natural system during this time must be taken into account when attempting to project future climatic scenarios (IPCC, 2013). Identifying the causes of this variability, as well as the mechanisms transferring it from one region to another, is crucial if we are to gain an overall understanding of the system.

The Western Mediterranean is an essential region as regards determining climatic teleconnections with the North Atlantic area (Cacho et al., 1999; Martrat et al., 2004; Sierro et al., 2005). Current sea-level, temperature and precipitation variability in the Western Mediterranean have been linked to the fluctuation of the atmospheric gradient formed by the Azores high- and the Icelandic low- pressure centers: the North Atlantic Oscillation (NAO) (Lionello et al., 2006; Tsimplis and Josey, 2001), a natural mode of atmospheric variability that has a pronounced effect on the climate of western central Europe at decadal time scales (Hurrell, 1995). The intensity of a NAO-like pattern has already been suggested as a

likely driving mechanism for several short-term environmental oscillations in the Western Mediterranean during the Holocene (Fletcher et al., 2012; Fletcher and Zielhofer, 2011; Frigola et al., 2007; Goy et al., 2003; Jalut et al., 2000; Jalut et al., 1997). However, little evidence is available concerning the impact of short-term climatic oscillations on past ocean productivity in the Mediterranean Sea (Lionello, 2012) or regarding its probable connection with North Atlantic climatic processes. Within the generalized oligotrophic character of the Mediterranean Sea, the Alboran Sea is considered an exception, exhibiting quasi-permanent areas of upwelling (Sarhan et al., 2000) where local vertical mixing is the main factor controlling marine productivity (Dafner et al., 2003). Upwelling dynamics are steered by local hydrography and atmospheric circulation (García-Gorriz and Carr, 1999). The pattern is as follows: offshore upwelling associated with southward drifting of the Atlantic Jet (AJ), and wind-induced coastal upwelling on the shore, promoted by winds blowing along the Spanish coast (Sarhan et al., 2000). The semi-enclosed features of the Alboran Sea lead to partial isolation of these phenomena, making it an ideal region for the study of the impact of short-term climatic oscillations on ocean productivity. Its latitudinal position and its connection with the Atlantic Ocean also provide a reasonable area for the study of ocean-climate teleconnections between northern processes and lower latitudes.

Coccolithophores are Haptophyte algae with calcified scales (coccoliths). Living forms are one of the major oceanic primary producers, and they are strongly influenced by nutrient availability, dissolved CO_2 concentrations in sea water, and SST, among others (Thierstein and Young, 2004). Thus, fossil forms of coccoliths preserved in deep-sea sediments are commonly used as a widespread proxy to reconstruct some of these variables as well as productivity (Baumann and Freitag, 2004; Colmenero-Hidalgo et al., 2004; Flores et al., 2000; Flores et al., 1999; Giraudeau, 1992).

The main objective of the present study was to reconstruct past productivity in an upwelling area of the Alboran Sea during the Holocene and to elucidate the climatic and oceanographic mechanisms involved in past variations in productivity, especially those related to North Atlantic climatic and oceanographic dynamics. For this reason, we report here a marine productivity record reconstructed from fossil coccolithophores along with data on oxygen isotopes, alkenone-estimated SST and other organic biomarkers for the last 12 kyr and correlate them with data referring to paleoenvironmental variations.

Area of study: modern water masses and climatic dynamics

Core HER-GC-T1 was recovered off the coast of Malaga (Figure 1b) in the Alboran Sea (Western Mediterranean). This is a transitional region where Atlantic Water (AW) enters the Mediterranean Sea through the Strait of Gibraltar as a jet of water called the Atlantic Jet (AJ) (García Lafuente et al., 2000), and becomes two quasi-permanent anticyclonic gyres on its way to the east: the Western Anticyclonic Gyre (WAG) and the eastern one (EAG) (Heburn and La Violette, 1990). The interaction between AW and the more saline and warmer Mediterranean water (MW) results in the formation of a geostrophic front at the northern limit of the WAG, called the Alboran Front (where HER-GC-T1 is located) (Minas et al., 1991) (Figure 1b). Southward migrations of the AJ allow the water from below, relatively warm and fresh, to upwell in the study area (Sarhan et al., 2000) forming a high-productivity cell referred to here as the "Malaga cell".

(Insert_Figure_1)

At depth, water circulation may be simplified with a three-layer model: on the surface, the mixing of AW and MW forms the Modified Atlantic Water (MAW), occupying the photic zone (100-200 m). Below, Levantine Intermediate Water (LIW), formed in the eastern part of the Mediterranean Sea, flows at a depth of 200-600 m towards the Strait of Gibraltar. Below the LIW, Western Mediterranean Deep Water (WMDW) flows at 600-3000 m depth in the same direction (Millot, 1999). WMDW is formed in the open sea off the Gulf of Lions (Figure 1c) (MEDOCGROUP, 1970). This deep water convection has a thermohaline origin and is linked to buoyancy preconditions determined by the heat flux, which in turn is steered by the blowing winds: the Tramontana (northerlies) and/or Mistral (north-westerlies) (Font et al., 2007; Mertens and Schott, 1998; Rixen et al., 2005; Smith et al., 2008). These cold dry winds blowing over the area induce heat losses and the evaporation of the MAW, which becomes saltier and colder and finally sinks owing to its high density, to form the WMDW (Font et al., 2007).

Present climate conditions in the region are influenced by an atmospheric high-pressure center above the Azores archipelago in the Atlantic Ocean resulting in hot dry summers and wetter winters (Sumner et al., 2001). At decadal and inter-annual time-scales, climatic variability in the North Atlantic region is modulated by the NAO (Hurrell, 1995). Currently, winter anomalies of the NAO in the Mediterranean

have been shown to influence sea level variability (Tsimplis and Josey, 2001), wave climate (Cañellas et al., 2010) and temperature and precipitation trends to a significant extent (Lionello et al., 2006). The NAO has been suggested to exert an indirect influence on net water flux in the Strait of Gibraltar via its high correlation with regional evaporation, precipitation and runoff (Fenoglio-Marc et al., 2013). The winter-NAO has also been correlated with heat flux anomalies that determine the buoyancy preconditions of deep water convection in the Gulf of Lions (Rixen et al., 2005), although Josey et al. (2011), using a broader definition of winter (October-March), concluded that the NAO only plays a secondary role when other modes of variability related to the heat flux are considered.

Material and methods

We analyzed the top 183 cm of gravity core HER-GC-T1 (Lat. 36°22'12''N, Long. 4°17'57''W), recovered by the BIO Hesperides during the Hermesione research cruise in 2009, from a depth of 658.9 meters below sea level (mbsl). The sediments recovered are mainly composed of dark greenish-gray mud rich in planktonic foraminifers.

Age model

Radiocarbon ages were determined on six samples of selected foraminiferal shells using the accelerator mass spectrometry (AMS) technique (Table 1) at the Poznan Radiocarbon Laboratory and Woods Hole Oceanographic Institution. Conversion from radiocarbon ages to calibrated calendar years was performed using the OxCal 4.2 online software (Bronk Ramsey, 2008) and the Marine13 calibration dataset curve (Reimer et al., 2013), which includes a correction of 400 yr for the global marine reservoir effect. The regional difference from this global reservoir correction (ΔR) (Stuiver and Braziunas, 1993) proved to be -22± 35 years (Siani et al., 2000) and was also considered. The age model for the last 12 kyr was based on linear interpolation between these six calendar ages (Figure 2) performed with the AnalySeries Version 1.1 (Paillard et al., 1996). The average sedimentation rate was found to be 18.41 ± 5.4 $cm*kyr^{-1}$. All dates reported in the text are given in calendar ages BP.

(Insert_Figure_2)

Table 1. Age model for core HER-GC-T1. [a]Poznan Radiocarbon Laboratory. [b]Woods Hole Oceanographic Institution.

Radiocarbon (Sample/Laboratory code)	Foram Type	Depth (cm)	Radiocarbon Age (yr BP)	Calendar Age (2-sigma error range) (yr cal. BP)
SEC1_2/ Poz-53233[a]	*G. inflata*	2	440 ± 25	88±62
SEC1_21/OS-87586[b]	*G. inflata*	21	1,810 ± 25	1,379±54
SEC1_63/ Poz-53234[a]	*G. inflata*	63	4,175 ± 35	4,284±76
SEC2_17/ Poz-53235[a]	*G. inflata*	107	6,100 ± 40	6,550±68
SEC2_54/OS-87587[b]	*G. inflata* and *N. pachyderma*	144	7,350 ± 35	7,834±58
SEC3_12/ Poz-53236[a]	*N. pachyderma*	202	10,400 ± 60	11,539±162

Coccolithophore analysis and taxonomy

Eighty-five samples were taken systematically every 2-3 cm. The resulting sampling gives an average time resolution of ~140 years. Slides for micropaleontological analyses were prepared following the settling technique proposed by Flores and Sierro (1997). Qualitative and quantitative analyses were performed using a Nikon Eclipse 80-i petrographic microscope with a phase contrast device at 1000x magnification. Nannofossil census counts were based on at least 500 specimens identified in a first count, which is representative for studying the main species (Fatela and Taborda, 2002). In a second count, 25 fields of view were observed in order to avoid underestimation and/or overestimation of the taxa whose abundance was less than 1% in the first count. The Nannofossil Accumulation Rate (NAR) is given in numbers of coccoliths*cm^{-2}*kyr^{-1}, and was calculated in each sample by considering dry-sediment density, the sedimentation rate and the absolute abundance of each species (number of coccoliths*g^{-1}). The total NAR was interpreted as a proxy of primary productivity. Relative abundance (%) was also calculated. All taxa identified in this study have been reported previously for the sampling location (Álvarez et al., 2010; Weaver and Pujol, 1988). The "small *Gephyrocapsa"* group is integrated by all *Gephyrocapsa* specimens smaller than 3 µm (Flores et al., 1999). Along with *Emiliania huxleyi* (<4 µm), they were lumped together as "small placoliths". Other taxa identified in this study were *Gephyrocapsa muellerae*, *Gephyrocapsa oceanica*, *Helicosphaera carteri*, *Syracosphaera* spp. and *Florisphaera profunda* (as dominant taxa). The rare taxa identified were *Braarudosphaera bigelowii*, *Calcidiscus*

153 *leptoporus, Calciosolenia murrayi, Coccolithus pelagicus* subsp. *braarudii, Coccolithus pelagicus* subsp.
154 *pelagicus, Gephyrocapsa caribbeanica, Oolithotus fragilis, Pontosphaera* spp., *Rhabdosphaera*
155 *clavigera, Umbilicosphaera sibogae, Umbellosphaera* spp. and *Discosphaera tubifera*. The latter four
156 were lumped together as the warm-water group (WWG) owing to their common and relatively high
157 record in warm waters (McIntyre and Bé, 1967; Okada and Honjo, 1973). Taxa pertaining to older
158 stratigraphic levels (regularly older than the Pliocene in this study) were deposited again after their
159 resuspension and transport to the core location and were also counted as rare species and designated
160 "reworked specimens".

161 The preservation of the coccolithophore assemblages is good (little or no evidence of dissolution;
162 diagnostic features fully preserved) (Flores and Marino, 2002). Moreover, the NARs were transformed
163 into coccoliths*m^{-2}*day^{-1}. The results are comparable to the annual flux found by Bárcena et al. (2004) in
164 the same area for sediment-trap samples, showing that dissolution and taphonomic effects are negligible
165 in this core.

166 *Oxygen stable isotopes*

167 Up to 20 well-preserved specimens of the planktic foraminifer *Globigerina bulloides* were picked
168 from the >200 µm size fraction in 66 samples. The individuals were crushed, subjected to ultrasound and
169 cleaned with methanol before isotopic analyses were performed with a SIRA mass spectrometer equipped
170 with a VG isocarb common acid bath system at the University of Barcelona. Calibration to the Vienna
171 Pee Dee Belemnite (VPDB) standard scale (Coplen, 1996) was accomplished using the NBS-19 standard,
172 and analytical precision was better than 0.06 ‰ for $\delta^{18}O$.

173 *Molecular biomarkers*

174 A total of 86 samples, taken every 2-3 cm, were selected for the analysis of fossil organic compounds
175 (long chain alkenones, alcohols and hydrocarbons). The experimental procedures used are described in
176 Villanueva et al. (1997). Samples were analysed with a Varian Gas Chromatograph (GC) model 450, an
177 autoSampler 8400, a Cold On-Column (COC) Injector 1093 and a Flame Ionization Detector (FID). The
178 carrier gas was hydrogen (2.5 mL/min). C_{37} unsaturated alkenones (di-unsaturated and tri-unsaturated) are
179 synthesized by coccolithophorid flora. Their identification and quantification allow the calculation of the

$U^{k'}_{37}$ index, which was calibrated according to the equation proposed by Müller et al. (1998) in order to measure SST. The total concentration of C_{37} alkenones ($[C_{37:2}+C_{37:3}]$) was also calculated and is interpreted as a proxy for poor/good preservation of organic matter in deep sea sediments in relation to well/poorly ventilated deep waters (Cacho et al., 2002). The *n*-hexacosan-1-ol index was calculated through the relative ratio of *n*-hexacosan-1-ol ($C_{26}OH$) to the sum of ($C_{26}OH$) plus *n*-nonacosane (C_{29}). Since *n*-hexacosanol is more labile to degradation processes than *n*-nonacosane, decreases in the *n*-hexacosan-1-ol index can be interpreted as a higher ventilation of the deep basin. (Cacho et al., 2000).

Statistical approaches

In order to search for possible relationships between some of the proxies addressed here, statistical cross-correlation, which is suitable for temporal series, was carried out using PAST 3.01 software (Hammer, 2001). This method requires evenly sampled temporal data, which were interpolated regularly every 0.14 kyr (the lowest resolution among those from all of the records correlated).

Results

Calcareous nannoflora distribution

On average, small placoliths constitute up to 80% of the nannofossil assemblage (Figure 3). Their NAR records maximum values from 7.7 to 6.2 ka. *G. muellerae* (Figure 3) is the only species that records its highest NAR from 12 to 10.5 ka, followed by a decreasing trend from 10.5 ka onwards, interrupted only by higher values from 7.7 to 6.2 ka. The NAR of the WWG is scarce for the whole period studied, except from 7.7 to 6.4 ka when it records higher values (Figure 3). *F. profunda* and small *G. oceanica* exhibit similar general variability (Figure 3): a low NAR up to 7.7 ka, when a large peak is observed; from then onwards up-core, they record higher NAR values as well as large oscillations.

Reworked specimens are mainly constituted by Upper Cretaceous, Paleogene and Neogene specimens. On average the percent of this allochthonous group relative to autochthonous taxa (Fig. 3) is 0.7% for the whole record. However, it shows five peaks up to 1.6% at 7.0, 6.2, 5.0, 4.1 and 2.8 ka.

The total NAR (Figure 3) shows an increasing trend from 12.5 to 7.7 ka. From that time onwards up to 6.5 ka, it records its highest values followed by a decreasing trend up-core.

(Insert_Figure_3)

Sea-Surface Temperature

$U^{k'}_{37}$- SST (Figure 3) has its absolute minimum (14.6°C) at 12 ka, and its absolute maximum (20.1°C) at 8.9 ka. A decreasing trend is observed from 8.9 ka up-core, characterized by a generalized smooth internal variability. More specifically, short cooling events (up to 1°C) are seen centered at 11.5, 10.4, 8.5, 7.7, 5.3, and 0.8 ka.

(Insert_Figure_4)

Oxygen isotopic record

As from 12 ka (Figure 4c) this record tends to lower values, its absolute minimum being reached at 7.8 ka and its values varying up to 1.48 ‰ during that period. From 7.8 to 3.8 ka several slight depletions interrupt a trend to higher values, increasing by a total of 0.98 ‰. From 3.8 ka to the top, $\delta^{18}O$ tends towards slightly lower values, with a range of 0.43 ‰.

Total concentration of C_{37} alkenones and the n-hexacosan-1-ol index

The total concentration of C_{37} alkenones (Figure 4d) shows higher values from 12 to 9 ka. This record is affected by a decreasing trend up to 7.5 ka, and from that time onwards up-core it shows low values and little variability. The *n*-hexacosan-1-ol index (Figure 4e) tends towards lower values from 12 to 7.5 ka. After the absolute minimum recorded at 7.5 ka, a trend towards higher values is recorded up-core, punctuated by several depletions.

Discussion

General primary productivity and SST trends

Holocene productivity can be divided into three periods according to the total NAR variability (Figure 3): from 25.5 to 7.7 ka, characterised by low productivity and a slight increasing trend; from 7.7 to 6.2 ka, when productivity reached its highest values; and from 6.2 ka onwards, a period affected by lower productivity and a slight decreasing trend up-core.

Specifically from 12 to 10.5 ka, low SST values correspond to a high *G. muellerae* NAR and relative abundances and a low WWG NAR and relative abundances (Figure 3), customarily used as cold- and

warm-water proxies, respectively (McIntyre and Bé, 1967; Okada and Honjo, 1973; Weaver and Pujol, 1988).

The long-term cooling trend shown by the $U^{k'}_{37}$-SSTs from 9 ka during the Holocene is in agreement with the findings of Marchal et al. (2002) from the study of seven cores from the northeast Atlantic and the Mediterranean Sea. However, from 7.7 to 6.2 ka there is no agreement between the total NAR and the SST cooling trend, suggesting that factors other than SST would have controlled coccolithophore production and variability during that time. Specifically, the signal of WWG (Figure 3) results from the sum of all taxa with a preference for warm waters. This does not exclude the possibility that other environmental parameters such us salinity, nutrients, eddies and species-specific biogeography could affect their distribution and variability (Baumann et al., 2005) and hence their signal in palaeorecords.

Despite this general cooling trend, the *G. muellerae* NAR and relative abundances decrease from 6.2 ka up-core, showing similar variability to that of the small placoliths, which are eurythermal species linked to the presence of nutrients (Okada and Wells, 1997). Both taxa could have been controlled by the same factors since they show similar responses. Flores et al. (1997) found low abundances of *G. muellerae* after the early part of the last Pleniglacial (73.9 kyr) in the Western Mediterranean, suggesting that the affinity of this species for cold-water conditions is unclear. We suggest that the abundance of *G. muellerae* has been responding not only to colder waters but also to nutrient availability as from 7.7 ka.

The NAR and relative abundances of *F. profunda* (Figure 3) increase at 7.7 ka and undergo several high-amplitude oscillations up-core as from that time. This species inhabits the lower photic zone (LPZ) and is abundant under a deep nutricline and an upper photic zone (UPZ) impoverished in nutrients (Molfino and McIntyre, 1990), a characteristic that affected the water column in the Alboran Sea during several periods of the last 7.7 ka.

The general trends shown by the SST profile are similar to that shown by the $\delta^{18}O$ record (Figure 4). From 8.9 ka both profiles follow a decreasing trend in agreement with that of the insolation curve (Figure 4a) (Berger, 1978). This suggests that insolation could have played an important role from that time onwards along the Holocene as a long-term factor influencing the SST, which in turn would have had an important effect on the isotopic composition of oxygen recorded in foraminiferal shells.

With regard to deep basin conditions, a period of well-preserved organic matter from 12 to 9.5 ka can be deduced from the higher concentration of C_{37} alkenones (Figure 4d). This period coincides with the last part of the Organic Rich Layer (ORL-1) reported by Cacho et al. (2002) in the Alboran Sea due to an oxygen-depleted environment during the deglaciation. The preservation of organic matter declines until 7.5 ka, coherent with the gradual increase in deep water ventilation shown by the *n*-hexacosan-1-ol index (Figure 4e). From these conditions, we deduce a period of thermohaline reactivation that gradually decreases from 7.5 ka onwards. During this latter period, the preservation of the organic matter is relatively low, although a slight increasing trend up-core can be recognized in the total concentration of C_{37} alkenones, in agreement with the gradual reduction in deep water ventilation (Figure 4e), while, according to the total NAR, lower productivity affects the photic zone (Figure 3).

According to Fletcher et al. (2012), continental aridity is evidenced by polen analysis of the marine core MD95-2043 (Figure 1b and 4f). This record shows a decreasing abundance of Mediterranean and temperate pollen grains up-core, pointing to a gradual decline in forest mass and more arid conditions during the Holocene.

Short-term changes

The 7.7 ka event. At 7.7 ka there is a simultaneous increase in the NAR of all dominant taxa (Figure 3). The high sedimentation rate from 7.7 to 6.2 ka (Figure 2) is partly responsible for this increase in NARs, since these depend on the former for its calculation. Nevertheless, the absolute abundances (coccoliths*g^{-1}) of these taxa also reflect this sharp increase at that time (data not shown), from which it may be deduced that the simultaneous increase in the NAR at 7.7 ka is not an artifact of the sedimentation rate. In addition, *F. profunda* NAR shows several high-amplitude oscillations from 7.7 ka, pointing to successive periods of high productivity in the LPZ and therefore, a change in the configuration of the upper water column may be deduced from then onwards up-core. Because all taxa were affected, even though some of them have different and/or opposite ecological preferences (e.g. nutrient availability and SST), we argue that the same ecological factors (or at least one) control them. We propose an increase in the Atlantic inflow in the Western Mediterranean Sea, as shown by the maximum flooding of the Southern coast of Spain dated at 7.4 ka (Zazo et al., 1994), and the ensuing establishment of the WAG in the Alboran basin

as a possible cause for this simultaneous peak in all NAR profiles. Directly associated with the appearance of the WAG, the productive "Malaga cell" would have been settled at that time, implying a nutrient input that would favour the blooming of all species.

It is worth noting that at 7.5 ka the *n*-hexacosan-1-ol index records its absolute minimum coeval with low values of the total concentration of C_{37} alkenones (Figure 4d, e), pointing to a well-ventilated deep basin. In this regard, Naranjo et al. (2012) demonstrated that the intensification of the WAG is able to ventilate deep waters in the Alboran Sea. Rohling et al. (1995) reported the establishment of the WAG at around 8 ka from the interpretation of an abrupt faunal change in the planktic foraminiferal assemblage, also identified and dated by Pérez-Folgado et al. (2003) at 7.7 ka. A change in the benthic foraminiferal assemblage was also recognised by Melki et al. (2009) at 8 ka in the Gulf of Lions. Jimenez-Espejo et al. (2007) deduced a remarkable redox event in the Algero-Balearic basin between 7.5 and 7 ka, interpreted as the redoxcline reaching the seabed due to intensification of the thermohaline circulation. From the analyses of pollen records, Fletcher et al. (2012) reported a long-term decline in Mediterranean forest levels from 7.5 ka. Reviewing many palaeoenvironmental records from marine and continental sites in the study area, Cortés Sánchez et al. (2012), deduced a long-term environmental crisis due to sea-level rise and changes in the thermohaline circulation at that time. Based on our results, we suggest that the 7.7 ka event observed in the NAR records would correspond to the appearance of the "Malaga cell" as a consequence of the establishment of the WAG. Ultimately, this would have been due to a major inflowing AJ along with an intensification of the thermohaline circulation in the Western Mediterranean at that time.

Variability of the productive "Malaga cell". *The F. profunda* NAR and relative abundances show large oscillations from the proposed appearance of the "Malaga cell" onwards. The relative abundance of this species has classically been used as a nutricline depth indicator in palaeoceanographic reconstructions in low latitudes, where *F. profunda* shows high relative abundances and may have dominated the assemblages during some periods (Beaufort et al., 1997; Flores et al., 2000; Incarbona et al., 2008; Molfino and McIntyre, 1990). In our records, *F. profunda* ranges up to 8% of the total assemblage and its average contribution (3.3%) is low, in agreement with sediment-trap analyses from the Alboran Sea (4%

and 2.5%) (Bárcena et al., 2004; Hernández-Almeida et al., 2011). Regarding relative abundances, the decrease/increase of one species may occur when other species increase/decrease, even though the absolute value of the former does not change. Because the changes in the relative abundance of *F. profunda* are of small magnitude, we interpret the NAR as a more suitable expression of *F. profunda* abundance and variability in this study. This species requires nutrients available in the LPZ (deeper nutricline) and low turbidity (lower productivity in the UPZ) (Ahagon et al., 1993) to allow light to reach the LPZ, and hence high values of *F. profunda* NAR can be suggested to represent these conditions. This argument is supported by the study of sediment-trap samples in the Alboran Sea, where the highest fluxes of *F. profunda* have been reported, along with water column stratification (Hernández-Almeida et al., 2011). Similarly, in a recent study carried out in Bay of Bengal, Mergulhao et al. (2013) linked high fluxes of *F. profunda* to a deep nutricline when oligotrophic conditions prevailed at the surface.

Conversely, the decreases in the *F. profunda* NAR were likely due to a shallower nutricline and/or higher turbulence in the UPZ, characteristic conditions of upwelling intensification. Small placoliths are a classic indicator of rich-nutrient waters in the UPZ (Okada and Wells, 1997). However, they show scarce variability from 7.7 ka onwards and, as is the case of the relative abundance of *F. profunda*, changes of small magnitude (Figure 3), and hence it is not possible to deduce periods of higher productivity from their record. Nevertheless, we argue that decreases in the *F. profunda* NAR would have been linked to the intensification of the upwelling conditions, as demonstrated by Ziveri et al. (1995) from the study of sediment-trap samples, where the lowest fluxes of *F. profunda* were linked to a shoaling of the nutricline during the upwelling period in southern California.

From this, we deduce that the high variability shown by *F. profunda* NAR points to pulses of weakening and intensification of upwelling conditions in the study area, implying that the semi-permanent nature of the productive ”Malaga cell” has characterized it for the last 7.7 kyr.

Upwelling intensity in the study area is linked to AJ dynamics (Sarhan et al., 2000). This implies that more factors would have influenced productivity, since these dynamics in turn are steered by the water exchange controlled hydraulically in the Strait of Gibraltar (García Lafuente et al., 2002). This water exchange determines a net water inflow at the Strait that compensates the freshwater loss at the sea-

surface induced by evaporation in the Mediterranean Sea (Fenoglio-Marc et al., 2013). With regard to outflow, this is essentially formed by the LIW and WMDW. The latter occupies the bottom layer and from the study of CTD profiles, the core location has been reported to have been under its direct influence (Ercilla, 2013, personal communication). Frigola et al. (2007) analyzed the UP10 fraction (fraction coarser than 10 μm) (Figure 5a) from marine core MD99-2343 (Figure 1c) and interpreted the occurrence of episodes of WMDW reinforcement in the Gulf of Lions for the last 12 kyr called the"Minorca events"(Table 2). There is a general correspondance between periods of maximum UP10 fraction and minimum *F. profunda* NAR, indicating a WMDW reinforcement in the Gulf of Lions coeval with intensification of the upwelling conditions in the Alboran Sea (Table 2, Figure 5). By contrast, during most of the periods in which the UP10 fraction records its lowest values, *F. profunda* NAR shows large peaks, indicating a relaxation of the upwelling and a more stable water column in the Alboran Sea during periods of WMDW weakening (Figure 5). The cross-correlation between the UP10 fraction and the NAR of *F. profunda* is R= -0.56, n= 85, p-value= 0.01 (correlation significant at 99%). This result highlights the notion that both proxies are anticorrelated at a moderate value. Because Holocene climate records are imperfect proxies for processes containing complicated mixtures of periodic and random signals (Thomson, 1990), complex effects difficult to identify, isolate and remove, can affect the correlation parameter. In addition, owing to chronological uncertainties another significant concern arises when comparing records based on different age models. Thus, it is important to bear in mind that this relatively moderate correlation value results from proxies of different nature (physical and biological), which were measured in different cores from adjacent basins.

(Insert_Figure_5)

Table 2. Timing of Minorca Events (WMDW reinforcement) in the Gulf of Lions (Frigola et al., 2007) and timing of the lower values of *F. profunda* NAR in the Alboran Sea.

Minorca Event	WMDW reinforcement periods in Frigola et al. (2007)	*F. profunda* NAR decreases in the Alboran Sea
	Age interval (ka cal BP)	Age interval (ka cal BP)

M8	9.0-7.8	9.2-7.8
M7	7.4-6.9	7.4-6.9
M6	6.5-5.8	6.6-6.1
M5	5.3-4.7	5.7-4.7
M4	4.2-4.0	4.2-3.1
M3	3.4-3.1	
M2	2.6-2.3	2.6-2.1
M1	1.8-1.4	
M0	0.8-0.2	0.9-0.2

According to García-Lafuente et al. (2007), the seasonal cycle of the outflow is linked to that of the annual formation of WMDW. The same authors (2002) demonstrated that the inflow and outflow fluctuate in-phase. In light of this, it could be suggested that a reinforcement of WMDW would have been simultaneous to an enhanced Atlantic inflow in order to compensate the evaporative losses that promoted WMDW formation. Changes in the AJ velocity forced a change in its incoming direction as follows: higher velocities would have forced the AJ to migrate southward and, as a consequence, upwelling would have occurred offshore since a volume of uplifted waters replaced the space left behind; conversely, lower velocities would have caused the northward displacement of the AJ and the development of the WAG (Cheney and Doblar, 1982; Sarhan et al., 2000; Vargas-Yáñez et al., 2002).

The SST short-term variability shows changes of small amplitude (up to 1 ºC) that coincide with most of the six short cooling events (1-1.5 ºC) recognized by Cacho et al. (2001) in a $U^{k'}_{37}$- SST record from the Alboran Sea. Cacho et al. (2001) studied these cooling events along a longitudinal transect, and observed that their amplitude was larger eastward. The authors argued that these were transmitted by North Atlantic inflowings but were amplified across the Mediterranean by strong winter winds. Taking into account the location of core HER-GC-T1 in this transect, the smaller magnitude of the SST cooling events is in agreement with the Mediterranean amplification effect reported by Cacho et al. (2001).

379 At millenial-centennial time-scale, SST and $\delta^{18}O$ variations are not simultaneous. Owing to the
380 oxygen isotope ratios within shells of *G. bulloides* are a function of the local temperature in which the
381 shells forms and the variations in continental ice sheets (Emiliani, 1955), discrepancies between both
382 records may be related to surface water salinity changes and/or ecological repercussions from the
383 different planktic groups employed (i.e. the different depths at which *G. bulloides* calcifies and alkenones
384 are produced).

385 The five largest peaks shown by the reworked specimens (Figure 5d) may be negligible owing to their
386 low relative abundance (up to 1.6%). Nevertheless, we submit that they could have paleosignificance
387 related to the processes described below due to their correspondence with periods of WMDW formation
388 (Figure 5). In the study area, reworked specimens have been linked to terrigenous input from exposed
389 continental margins and fluctuation in the sea level (Colmenero-Hidalgo et al., 2004; Flores et al., 1997).
390 We discard this hypothesis since the estimated changes in relative mean sea levels during the Holocene
391 did not exceed 1.3 m in the Alboran Sea (Goy et al., 2003). Nevertheless, reworked specimens can be also
392 transported by rivers flowing into the study area (Guadalfeo River and Guadalhorce River (Figure 1b)).
393 Southward migrations of the North Atlantic westerlies (i.e. blowing over the Gulf of Lions) allows the
394 penetration of winter storm tracks in the Mediterranean region. This was observed for the Holocene by
395 Fletcher et al. (2012), who linked southward displacements of the North Atlantic westerlies with forest
396 expansion in the Western Mediterranean. Higher precipitation during times of prevailing westerlies would
397 have involved enhanced fluvial discharges, supporting the transport of reworked specimens by rivers
398 during periods of WMDW formation.

399 The several changes seen in the *n*-hexacosan-1-ol index (Figure 5c) do not reveal any evident
400 correlation with those of the UP10 fraction. It is expected that after its formation the WMDW would have
401 ventilated the seafloor on its way to the Strait. However, fluvial discharges in the study area during those
402 periods could have partly masked the short-term ventilation signal shown by the *n*-hexacosan-1-ol index.

403 From these results, we propose a two-phase scenario to explain the behavior of the productive Malaga
404 cell at millenial-centennial time-scale from its appearance at 7.7 ka: [1] more arid climate conditions and
405 weaker northerlies/north-westerlies in the Gulf of Lions, the latter leading to a reduction in WMDW

406 formation concurrent with a weakening of the AJ inflow. This would have promoted a reduction in
407 vertical mixing (Figure 6a), triggering a weakening of the upwelling conditions and leading to a more
408 stable water column in the Alboran Sea; [2] wetter climate conditions and an intensification of
409 northerly/north-westerly winds in the Gulf of Lions would have prompted a WMDW reinforcement
410 simultaneous with a stronger AJ and its southward migration. This would have caused an increase in
411 vertical mixing, leading to an intensification of the upwelling conditions in the Alboran Sea (Figure 6b).
412 *Proposed forcing mechanism.*
413 Atmospheric pressure over the Mediterranean is the main driving force of water exchange in the
414 Strait (García Lafuente et al., 2002) as well as of the wind intensity, which determines the WMDW
415 formation (Leaman and Schott, 1991; Rixen et al., 2005). On a longer time-scale, a NAO-like mode of
416 atmospheric circulation could represent a mechanism influencing climate variability and productivity at a
417 millenial-centennial time-scale in the study area due to the well-known climatic teleconnection of the
418 Western Mediterranean with northern latitudes (Cacho et al., 1999; Martrat et al., 2004). This relationship
419 has already been suggested by several authors (Fletcher et al., 2012; Frigola et al., 2007; Goy et al., 2003;
420 Moreno et al., 2004; Sánchez-Goñi et al., 2002), although the interpretations are limited by the absence of
421 a robust paleo-NAO reconstruction. Trouet et al. (2009) reconstructed the winter-NAO circulation pattern
422 for the past 900 years, and later, Olsen et al. (2012) expanded it to 5,200 years (Figure 7). A comparison
423 between the winter-NAO reconstruction and the UP10 fraction by Frigola et al. (2007) reveals a good
424 visual match (Figure 7b), supported by the reasonable value of its cross-correlation: R= 0.60, n=45, p
425 value= 0.002.
426 (Insert_Figure_6)
427 Trouet et al. (2009) and Olsen et al. (2012) also inferred the NAO index (Figure 7a), which is the
428 normalized December-to-March sea-level pressure between the Azores high- and the Icelandic low-
429 pressure centers, expressed as a bipolar circulation pattern. Previous work suggests that
430 northerly/westerly winds over the Gulf of Lions as well as enhanced precipitation in the Western
431 Mediterranean would have been triggered during negative NAO-like conditions (Combourieu Nebout et
432 al., 2002; Fletcher et al., 2012; Roberts et al., 2012; Trigo et al., 2004). However, a firm relationship

between the timing of periods of intensified upwelling conditions in the Alboran Sea and bimodality in the winter-NAO phases cannot be established from their comparison (Figure 7, dark bars). Nevertheless, we propose the winter-NAO as a likely forcing mechanism directly involved in the intensity of northerly/north-westerly winds that drove WMDW formation, a physical process that here is in turn proposed to be related to the variability of the "Malaga cell" since its appearance at 7.7 ka .

(Insert_Figure_7)

Conclusions

Down-core variations in the NAR are tightly linked to changes in marine paleoproductivity. A dramatic change observed in the NAR of all coccolithophore taxa at 7.7 ka has been related to a prominent fast-flowing AJ and the ensuing establishment of the WAG. These conditions would have favoured the establishment of the semi-permanent productive "Malaga cell" at 7.7 ka. From that time throughout the Holocene, the area was affected by a general cooling trend, as revealed by alkenone-estimated SST. Nannofossil records point to a general decreasing trend in productivity, altered by higher variability based on the alternation of events of weakened and intensified upwelling conditions since the establishment of the "Malaga cell". These variations in productivity have been found to be synchronous with periods of WMDW reinforcement in the Gulf of Lions, in such a way that whenever WMDW formation was strengthened, a productive event would have occurred in the Alboran Sea.

A two-phase scenario (Figure 6) is proposed to describe the main climatic and oceanographic features prevailing in the Western Mediterranean along the Holocene at millennial-centennial time-scale: phase [1] together with more arid climate conditions, weaker northerly/north-westerly winds would have resulted in a reduction in WMDW formation in the Gulf of Lions, which would have coincided with a minor AJ influx. As a result, a weakening of the upwelling conditions would occur and a stable water colum would have characterized the study area; phase [2] together with wetter climate conditions, stronger northerlies/north-westerlies blowing over the Gulf of Lions would have driven a major WMDW formation simultaneous to an enhancement of the AJ influx that would have migrated southward. This would have prompted vertical mixing in the study area intensifying upwelling conditions.

The winter-NAO circulation pattern has proved to be a highly influential mechanism in the processes explained by both phases. These results highlight the sensitivity of the Western Mediterranean to high-latitude climatic systems and point to the "Malaga cell" as a location of high interest in the Alboran Sea, since it provides an information that in turn can be used to unravel the climatic and oceanographic patterns that characterized the Western Mediterranean in the past.

Acknowledgements

We thank two anonymous reviewers for their valuable contribution to improve this manuscript. B. Ausín is grateful to Y. González and B. Hortelano (Department of Environmental Chemistry, IDAEA-CSIC, Barcelona) for their guidance and supervision during the geochemical analyses. We thank G. Ercilla and J. Salat for their valuable comments and suggestions. This study was supported by FPU grant AP2010-2559 from the Ministry of Education of Spain awarded to B. Ausín and by the Consolider Ingenio "GRACCIE" CSD 2007-00067 program, the CGL2011-26493 program and the VACLIODP339 and MINECO CTM2012-38248 projects of the Spanish Ministry of Science and Innovation.

All original data in this study necessary to understand, evaluate and replicate this research are accessible via correspondence with the main author, who will willingly make them available for free to anyone upon request.

References

Ahagon N, Tanaka Y and Ujiié H. (1993) Florisphaera profunda, a possible nannoplankton indicator of late Quaternary changes in sea-water turbidity at the northwestern margin of the Pacific. *Marine Micropaleontology* 22: 255-273.

Álvarez C, Amore FO, Cros L, et al. (2010) Coccolithophore biogeography in the Mediterranean Iberian margin. *Revista Española de Micropaleontología* 42: 359-372.

Bárcena MA, Flores JA, Sierro FJ, et al. (2004) Planktonic response to main oceanographic changes in the Alboran Sea (Western Mediterranean) as documented in sediment traps and surface sediments. *Marine Micropaleontology* 53: 423-445.

Baumann K-H and Freitag T. (2004) Pleistocene fluctuations in the northern Benguela Current system as revealed by coccolith assemblages. *Marine Micropaleontology* 52: 195-215.

Baumann KH, Andruleit H, Boeckel B, et al. (2005) The significance of extant coccolithophores as indicators of ocean water masses, surface water temperature, and palaeoproductivity: a review. *Palaeontologische Zeitschrift* 79: 93-112.

Beaufort L, Lancelot Y, Camberlin P, et al. (1997) Insolation Cycles as a Major Control of Equatorial Indian Ocean Primary Production. *Science* 278: 1451-1454.

Berger A. (1978) Long-Term Variations of Daily Insolation and Quaternary Climatic Changes. *Journal of the Atmospheric Sciences* 35: 2362-2367.

494 Bronk Ramsey C. (2008) Deposition models for chronological records. *Quaternary Science Reviews* 27:
495 42-60.
496 Cacho I, Grimalt JO and Canals M. (2002) Response of the Western Mediterranean Sea to rapid climatic
497 variability during the last 50,000 years: a molecular biomarker approach. *Journal of Marine*
498 *Systems* 33-34: 253-272.
499 Cacho I, Grimalt JO, Canals M, et al. (2001) Variability of the western Mediterranean Sea surface
500 temperature during the last 25,000 years and its connection with the Northern Hemisphere
501 climatic changes. *Paleoceanography* 16: 40-52.
502 Cacho I, Grimalt JO, Pelejero C, et al. (1999) Dansgaard-Oeschger and Heinrich Event Imprints in
503 Alboran Sea Paleotemperatures. *Paleoceanography* 14: 698-705.
504 Cacho I, Grimalt JO, Sierro FJ, et al. (2000) Evidence for enhanced Mediterranean thermohaline
505 circulation during rapid climatic coolings. *Earth and Planetary Science Letters* 183: 417-429.
506 Cañellas B, Orfila Förster A, Méndez Incera F-J, et al. (2010) Influence of the NAO on the northwestern
507 Mediterranean wave climate. *Scientia Marina* 74: 55-64.
508 Colmenero-Hidalgo E, Flores J-A, Sierro FJ, et al. (2004) Ocean surface water response to short-term
509 climate changes revealed by coccolithophores from the Gulf of Cadiz (NE Atlantic) and Alboran
510 Sea (W Mediterranean). *Palaeogeography, Palaeoclimatology, Palaeoecology* 205: 317-336.
511 Combourieu Nebout N, Turon JL, Zahn R, et al. (2002) Enhanced aridity and atmospheric high-pressure
512 stability over the western Mediterranean during the North Atlantic cold events of the past 50 k.y.
513 *Geology* 30: 863-866.
514 Coplen TB. (1996) Editorial: More uncertainty than necessary. *Paleoceanography* 11: 369-370.
515 Cortés Sánchez M, Jiménez Espejo FJ, Simón Vallejo MD, et al. (2012) The Mesolithic-Neolithic
516 transition in southern Iberia. *Quaternary Research* 77: 221-234.
517 Cheney RE and Doblar RA. (1982) Structure and variability of the alboran sea frontal system. *Journal of*
518 *Geophysical Research: Oceans* 87: 585-594.
519 Dafner EV, Boscolo R and Bryden HL. (2003) The N:Si:P molar ratio in the Strait of Gibraltar.
520 *Geophysical Research Letters* 30: 1506.
521 Emiliani C. (1955) Pleistocene temperatures. *Geology* 63: 539-578.
522 Fatela F and Taborda R. (2002) Confidence limits of species proportions in microfossil assemblages.
523 *Marine Micropaleontology* 45: 169-174.
524 Fenoglio-Marc L, Mariotti A, Sannino G, et al. (2013) Decadal variability of net water flux at the
525 Mediterranean Sea Gibraltar Strait. *Global and Planetary Change* 100: 1-10.
526 Fletcher WJ, Debret M and Sanchez Goñi MF. (2012) Mid-Holocene emergence of a low-frequency
527 millennial oscillation in western Mediterranean climate: Implications for past dynamics of the
528 North Atlantic atmospheric westerlies. *The Holocene* 23: 153-166.
529 Fletcher WJ and Zielhofer C. (2011) Fragility of Western Mediterranean landscapes during Holocene
530 Rapid Climate Changes. *CATENA*.
531 Flores JA, Bárcena MA and Sierro FJ. (2000) Ocean-surface and wind dynamics in the Atlantic Ocean off
532 Northwest Africa during the last 140 000 years. *Palaeogeography, Palaeoclimatology,*
533 *Palaeoecology* 161: 459-478.
534 Flores JA, Gersonde R and Sierro FJ. (1999) Pleistocene fluctuations in the Agulhas Current
535 Retroflection based on the calcareous plankton record. *Marine Micropaleontology* 37: 1-22.
536 Flores JA and Marino M. (2002) Pleistocene calcareous nannofossil stratigraphy for ODP Leg 177
537 (Atlantic sector of the Southern Ocean) *Marine Micropaleontology* 45: 191-224.
538 Flores JA and Sierro FJ. (1997) Revised technique for calculation of calcareous nannofossil accumulation
539 rates. *Micropaleontology* 43: 321-324.
540 Flores JA, Sierro FJ, Francés G, et al. (1997) The last 100,000 years in the western Mediterranean: sea
541 surface water and frontal dynamics as revealed by coccolithophores. *Marine Micropaleontology*
542 29: 351-366.
543 Font J, Palanques A, Puig P, et al. (2007) Sequence of hydrographic changes in NW Mediterranean deep
544 water due to the exceptional winter of 2005. *Scientia Marina* 71: 339-346.
545 Frigola J, Moreno A, Cacho I, et al. (2007) Holocene climate variability in the western Mediterranean
546 region from a deepwater sediment record. *Paleoceanography* 22: PA2209.

García-Gorriz E and Carr ME. (1999) The climatological annual cycle of satellite-derived phytoplankton pigments in the Alboran Sea: a physical interpretation. *Geophys. Res. Lett.*

García Lafuente J, Álvarez Fanjul E, Vargas JM, et al. (2002) Subinertial variability in the flow through the Strait of Gibraltar. *Journal of Geophysical Research: Oceans* 107.

García Lafuente J, Sánchez Román A, Díaz del Río G, et al. (2007) Recent observations of seasonal variability of the Mediterranean outflow in the Strait of Gibraltar. *Journal of Geophysical Research: Oceans* 112: C10005.

García Lafuente J, Vargas JM, Plaza F, et al. (2000) Tide at the eastern section of the Strait of Gibraltar. *Journal of Geophysical Research: Oceans* 105: 14197-14213.

Giraudeau J. (1992) Distribution of Recent nannofossils beneath the Benguela system: Southwest African continental margin. *Marine Geology* 108: 219-237.

Goy JL, Zazo C and Dabrio CJ. (2003) A beach-ridge progradation complex reflecting periodical sea-level and climate variability during the Holocene (Gulf of Almería, Western Mediterranean). *Geomorphology* 50: 251-268.

Hammer Ø, Harper, D.A.T., Ryan, P.D. (2001) PAST: Paleontological statistics software package for education and data analysis. *Palaeontologia Electronica* 4: 9.

Heburn GW and La Violette PE. (1990) Variations in the Structure of the Anticyclonic Gyres Found in the Alboran Sea. *Journal of Geophysical Research* 95: 1599-1613.

Hernández-Almeida I, Bárcena MA, Flores JA, et al. (2011) Microplankton response to environmental conditions in the Alboran Sea (Western Mediterranean): One year sediment trap record. *Marine Micropaleontology* 78: 14-24.

Hurrell JW. (1995) Decadal Trends in the North Atlantic Oscillation: Regional Temperatures and Precipitation. *Science* 269: 676-679.

Incarbona A, Di Stefano E, Patti B, et al. (2008) Holocene millennial-scale productivity variations in the Sicily Channel (Mediterranean Sea). *Paleoceanography* 23: PA3204.

IPCC. (2013) IPCC, 2013: Climate Change 2013: The Physical Science Basis. Contribution of Working Group I to the Fifth Assessment Report of the Intergovernmental Panel on Climate Change In: Stocker TF, D. Qin, G.-K. Plattner, M. Tignor, S.K. Allen, J. Boschung, A. Nauels, Y. Xia, V. Bex and P.M. Midgley (ed) *Cambridge University Press.* Cambridge, United Kingdom and New York, NY, USA,, 1535 pp.

Jalut G, Esteban Amat A, Bonnet L, et al. (2000) Holocene climatic changes in the Western Mediterranean, from south-east France to south-east Spain. *Palaeogeography, Palaeoclimatology, Palaeoecology* 160: 255-290.

Jalut G, Esteban Amat A, Riera i Mora S, et al. (1997) Holocene climatic changes in the western Mediterranean: installation of the Mediterranean climate. *Comptes Rendus de l'Académie des Sciences - Series IIA - Earth and Planetary Science* 325: 327-334.

Jimenez-Espejo FJ, Martinez-Ruiz F, Sakamoto T, et al. (2007) Paleoenvironmental changes in the western Mediterranean since the last glacial maximum: High resolution multiproxy record from the Algero-Balearic basin. *Palaeogeography, Palaeoclimatology, Palaeoecology* 246: 292-306.

Josey SA, Somot S and Tsimplis M. (2011) Impacts of atmospheric modes of variability on Mediterranean Sea surface heat exchange. *Journal of Geophysical Research: Oceans* 116: C02032.

Leaman KD and Schott FA. (1991) Hydrographic Structure of the Convection Regime in the Gulf of Lions: Winter 1987. *Journal of Physical Oceanography* 21: 575-598.

Lionello P. (2012) *The Climate of the Mediterranean Region: From the past to the future*, Burlington: Elsevier Science.

Lionello P, Manotte-Rizzoli P and Boscolo R. (2006) Relations between Variability in the Mediterranean Region and Mid-Latitude Variability. In: Elsevier (ed) *Mediterranean Climate Variability.* Amsterdam, 179-226.

Marchal O, Cacho I, Stocker TF, et al. (2002) Apparent long-term cooling of the sea surface in the northeast Atlantic and Mediterranean during the Holocene. *Quaternary Science Reviews* 21: 455-483.

599 Martrat B, Grimalt JO, Lopez-Martinez C, et al. (2004) Abrupt Temperature Changes in the Western
600 Mediterranean over the Past 250,000 Years. *Science* 306: 1762-1765.
601 Mayewski PA, Rohling EE, Curt Stager J, et al. (2004) Holocene climate variability. *Quaternary*
602 *Research* 62: 243-255.
603 McIntyre A and Bé AWH. (1967) Modern coccolithophoridae of the Atlantic Ocean. Placoliths and
604 cyrtoliths. *Deep Sea Research and Oceanographic Abstracts* 14: 561-597.
605 MEDOCGROUP. (1970) Observation of formation of deep water in the Mediterranean Sea, 1969. *Nature*
606 227: 1037-1040.
607 Melki T, Kallel N, Jorissen FJ, et al. (2009) Abrupt climate change, sea surface salinity and
608 paleoproductivity in the western Mediterranean Sea (Gulf of Lion) during the last 28 kyr.
609 *Palaeogeography, Palaeoclimatology, Palaeoecology* 279: 96-113.
610 Mergulhao LP, Guptha MVS, Unger D, et al. (2013) Seasonality and variability of coccolithophore fluxes
611 in response to diverse oceanographic regimes in the Bay of Bengal: Sediment trap results.
612 *Palaeogeography, Palaeoclimatology, Palaeoecology* 371: 119-135.
613 Mertens C and Schott F. (1998) Interannual Variability of Deep-Water Formation in the Northwestern
614 Mediterranean. *Journal of Physical Oceanography* 28: 1410-1424.
615 Millot C. (1999) Circulation in the Western Mediterranean Sea. *Journal of Marine Systems* 20: 423-442.
616 Minas HJ, Coste B, Le Corre P, et al. (1991) Biological and Geochemical Signatures Associated With the
617 Water Circulation Through the Strait of Gibraltar and in the Western Alboran Sea. *Journal of*
618 *Geophysical Research* 96: 8755-8771.
619 Molfino B and McIntyre A. (1990) Precessional forcing of nutricline dynamics in the equatorial Atlantic.
620 *Science* 249: 766-769.
621 Moreno A, Cacho I, Canals M, et al. (2004) Millennial-scale variability in the productivity signal from
622 the Alboran Sea record, Western Mediterranean Sea. *Palaeogeography, Palaeoclimatology,*
623 *Palaeoecology* 211: 205-219.
624 Müller PJ, Kirst G, Ruhland G, et al. (1998) Calibration of the alkenone paleotemperature index U37K'
625 based on core-tops from the eastern South Atlantic and the global ocean (60°N-60°S).
626 *Geochimica et Cosmochimica Acta* 62: 1757-1772.
627 Naranjo C, García Lafuente J, Sánchez Garrido JC, et al. (2012) The Western Alboran Gyre helps
628 ventilate the Western Mediterranean Deep Water through Gibraltar. *Deep Sea Research Part I:*
629 *Oceanographic Research Papers* 63: 157-163.
630 Okada H and Honjo S. (1973) The distribution of oceanic coccolithophorids in the Pacific. *Deep Sea*
631 *Research and Oceanographic Abstracts* 20: 355-374.
632 Olsen J, Anderson NJ and Knudsen MF. (2012) Variability of the North Atlantic Oscillation over the past
633 5,200 years. *Nature Geosciences* 5: 808-812.
634 Paillard D, Labeyrie L and Yiou P. (1996) Macintosh program performs time-series analysis. *Eos Trans.*
635 *AGU* 77: 379.
636 Reimer PJ, Bard E, Bayliss A, et al. (2013) IntCal13 and Marine13 Radiocarbon Age Calibration Curves
637 0-50,000 Years cal BP. Radiocarbon,. *Radiocarbon* 55.
638 Rixen M, Beckers JM, Levitus S, et al. (2005) The Western Mediterranean Deep Water: A proxy for
639 climate change. *Geophysical Research Letters* 32: L12608.
640 Roberts N, Moreno A, Valero-Garcés BL, et al. (2012) Palaeolimnological evidence for an east-west
641 climate see-saw in the Mediterranean since AD 900. *Global and Planetary Change* 84-85: 23-
642 34.
643 Rohling EJ, Den Dulk M, Pujol C, et al. (1995) Abrupt hydrographic change in the Alboran Sea (western
644 Mediterranean) around 8000 yrs BP. *Deep Sea Research Part I: Oceanographic Research*
645 *Papers* 42: 1609-1619.
646 Sánchez-Goñi M, Cacho I, Turon J, et al. (2002) Synchroneity between marine and terrestrial responses to
647 millennial scale climatic variability during the last glacial period in the Mediterranean region.
648 *Climate Dynamics* 19: 95-105.
649 Sarhan T, García Lafuente J, Vargas M, et al. (2000) Upwelling mechanisms in the northwestern Alboran
650 Sea. *Journal of Marine Systems* 23: 317-331.

Siani G, Paterne M, Arnold M, et al. (2000) Radiocarbon reservoir ages in the Mediterranean Sea and Black Sea *Radiocarbon* 42: 271-280.
Sierro FJ, Hodell DA, Curtis JH, et al. (2005) Impact of iceberg melting on Mediterranean thermohaline circulation during Heinrich events. *Paleoceanography* 20: PA2019.
Smith RO, Bryden HL and Stansfield K. (2008) Observations of new western Mediterranean deep water formation using Argo floats 2004-2006. *Ocean Science* 2: 133-149.
Stuiver M and Braziunas TF. (1993) 14C Ages of Marine Samples to 10,000 BC *Radiocarbon* 35: 137-118.
Sumner G, Homar V and Ramis C. (2001) Precipitation seasonality in eastern and southern coastal Spain. *International Journal of Climatology* 21: 219-247.
Thierstein HR and Young JR. (2004) Coccolithophores: from molecular processes to global impact. 565.
Thomson DJ. (1990) Time Series Analysis of Holocene Climate Data. *Philosophical Transactions of the Royal Society of London. Series A, Mathematical and Physical Sciences* 330: 601-616.
Trigo RM, Pozo-Vázquez D, Osborn TJ, et al. (2004) North Atlantic oscillation influence on precipitation, river flow and water resources in the Iberian Peninsula. *International Journal of Climatology* 24: 925-944.
Trouet V, Esper J, Graham NE, et al. (2009) Persistent Positive North Atlantic Oscillation Mode Dominated the Medieval Climate Anomaly *Science* 324: 78-80.
Tsimplis MN and Josey SA. (2001) Forcing of the Mediterranean Sea by atmospheric oscillations over the North Atlantic. *Geophysical Research Letters* 28: 803-806.
Vargas-Yáñez M, Plaza F, García-Lafuente J, et al. (2002) About the seasonal variability of the Alboran Sea circulation. *Journal of Marine Systems* 35: 229-248.
Villanueva J, Pelejero C and Grimalt JO. (1997) Clean-up procedures for the unbiased estimation of C37 alkenone sea surface temperatures and terrigenous n-alkane inputs in paleoceanography. *Journal of Chromatography A* 757: 145-151.
Wanner H, Solomina O, Grosjean M, et al. (2011) Structure and origin of Holocene cold events. *Quaternary Science Reviews* 30: 3109-3123.
Weaver PPE and Pujol C. (1988) History of the last deglaciation in the Alboran Sea (western Mediterranean) and adjacent north Atlantic as revealed by coccolith floras. *Palaeogeography, Palaeoclimatology, Palaeoecology* 64: 35-42.
Zazo C, Goy J-L, Somoza L, et al. (1994) Holocene sequence of sea-level fluctuations in relation to climatic trends in the Atlantic-Mediterranean linkage coast. *Journal of Coastal Research* 10: 933-945.
Ziveri P, Thunell RC and Rio D. (1995) Export production of coccolithophores in an upwelling region: Results from San Pedro Basin, Southern California Borderlands. *Marine Micropaleontology* 24: 335-358.

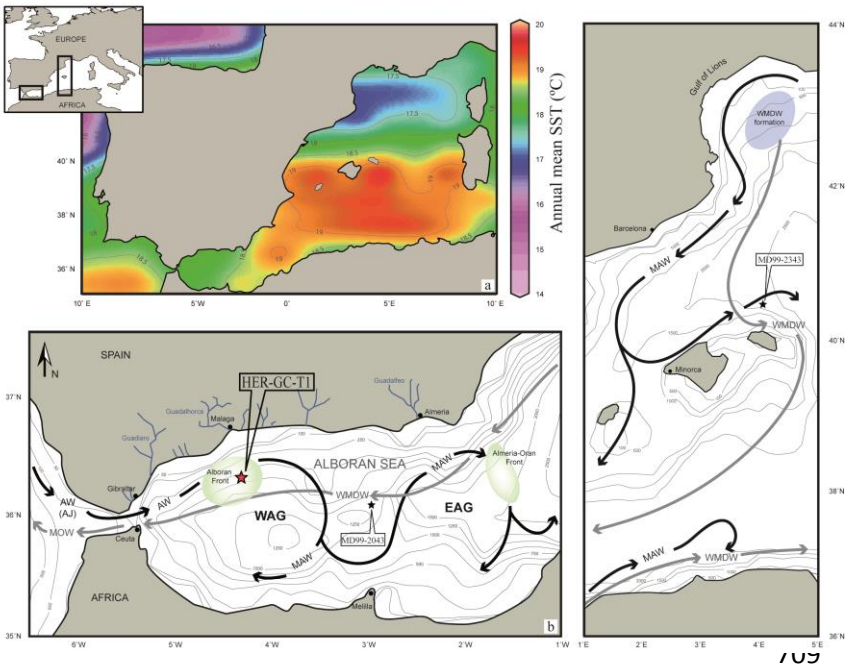

Figure 1. Study area. a) Map of the annual mean SST (ºC) in the Western Mediterranean Sea plotted with Ocean Data View (Brown, 1998). b) Study area and HER-GC-T1 core location in the Alboran Sea. c) Gulf of Lions area where WMDW formation occurs. Black arrows represent general superficial circulation. Grey arrows trace general deep circulation. AW: Atlantic Water, entering the Alboran Sea as the Atlantic Jet: AJ. MAW: Modified Atlantic Water. WMDW: Western Mediterranean Deep Water. MOW: Mediterranean Outflowing Water. WAG: Western Anticyclonic Gyre. EAG: Eastern Anticyclonic Gyre.

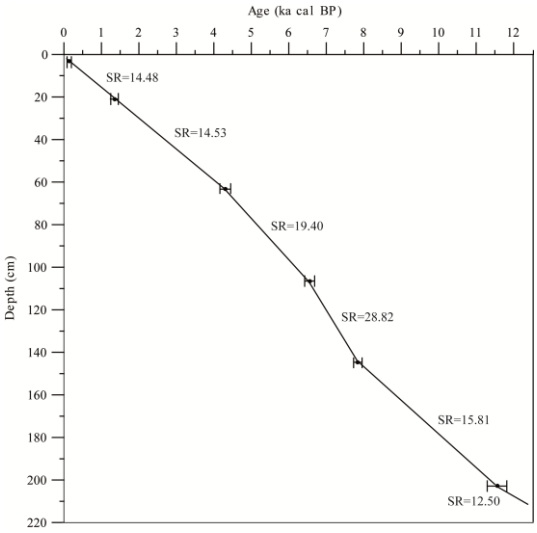

Figure 2. Age-depth model. Age control points are marked by a black dot and associated error bars. The solid line joining them is the age given in ka cal. BP. SR stands for sedimentation rate, given in $cm*kyr^{-1}$.

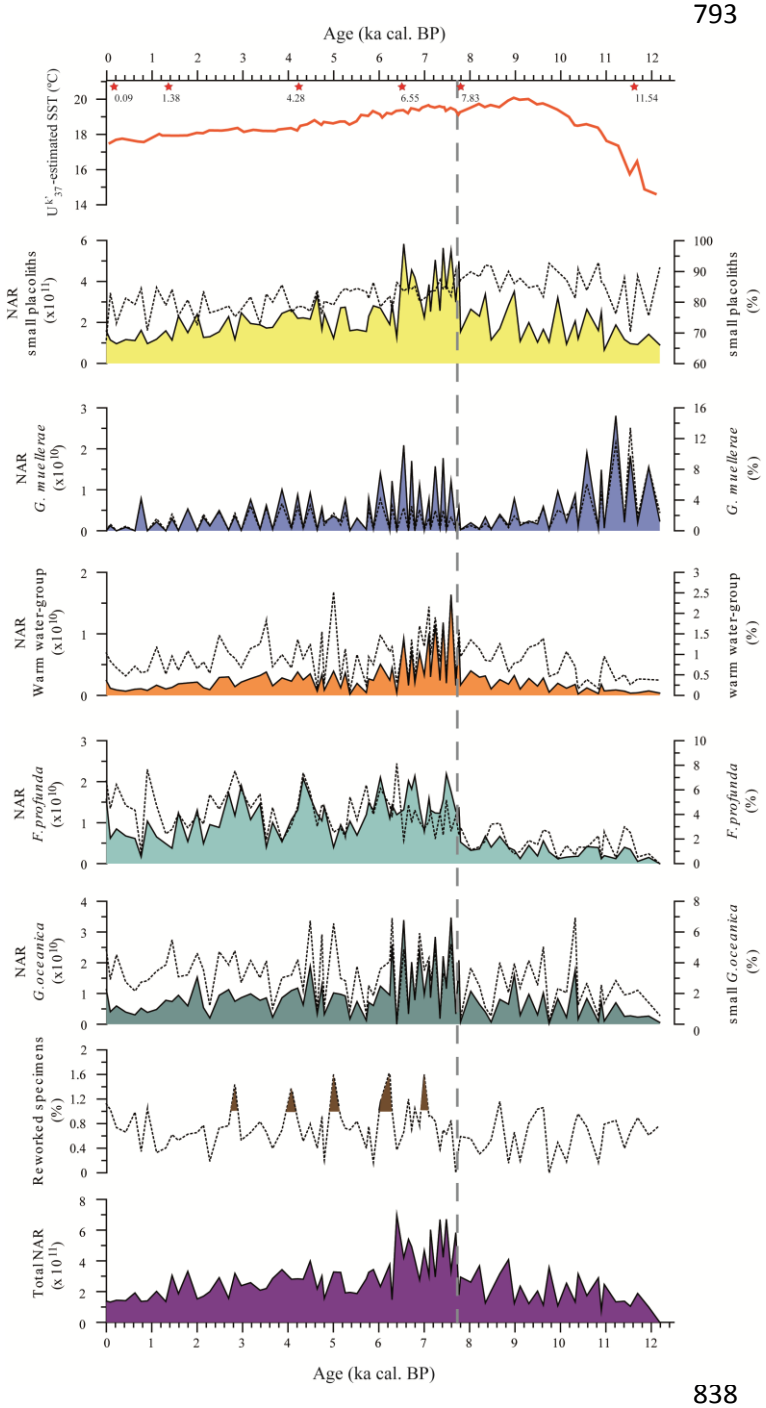

Figure 3. $U^{k'}_{37}$-estimated SST (°C). Nannofossil Accumulation Rate (NAR) (black lines) and relative abundance (%) (dashed line) of the coccolithophore assemblage. The grey dashed vertical line indicates the 7.7 ka cal. BP event. Red stars represent age control points (ka cal. BP) (Table 1).

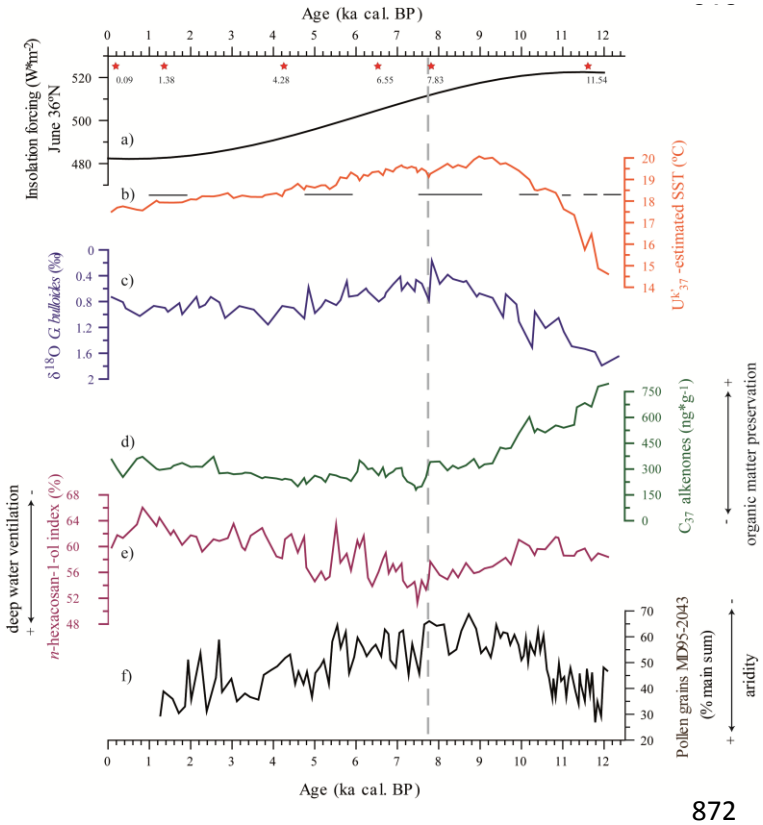

872

873 Figure 4 a) Insolation curve (June, 36° N) (Berger, 1978). b) $U^{k'}_{37}$-estimated SST (°C). Horizontal lines
874 mark the rapid Holocene cooling events identified by Cacho et al. (2001) c) $\delta^{18}O$ record (‰) (Note that
875 the vertical axis is reversed). d) Concentration of C_{37} alkenones ($[C_{37:2}+C_{37:3}]$) ($ng*g^{-1}$). e) *n*-hexacosan-1-
876 ol index (%). f) Pollen grains from core MD95-2043 in the Alboran Sea for all temperate and
877 Mediterranean forest taxa.(Fletcher et al., 2012).
878
879
880
881
882
883
884
885
886
887
888
889
890
891
892
893
894
895
896
897
898

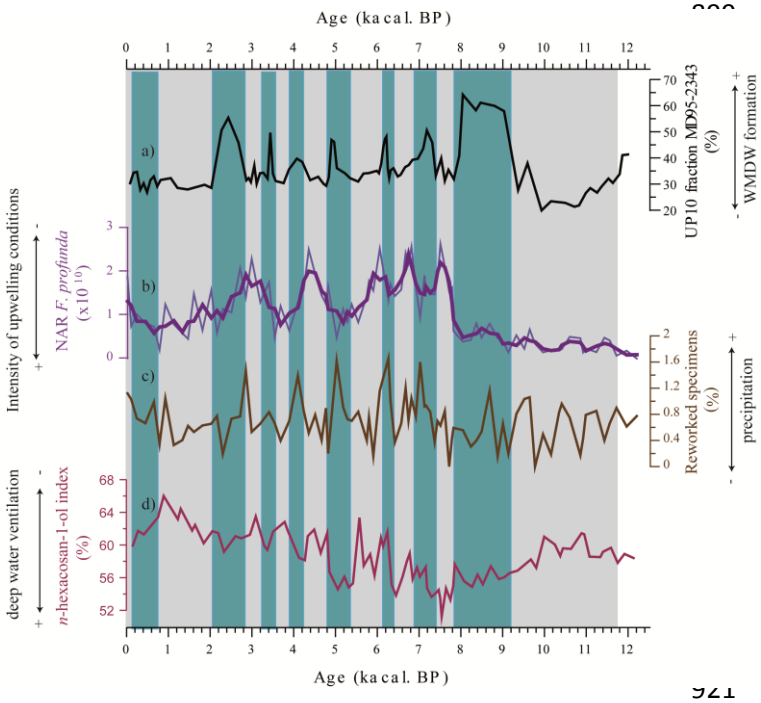

Figure 5. a) UP10 fraction record from core MD95-2343 north of Minorca (Frigola et al., 2007) (%). b) *F. profunda* NAR from core HER-GC-T1 (coccoliths*cm^{-2}*kyr^{-1}). The thin line represents original values while the thick line represents the original data fitted to a 3-point moving average smoothing spline. c) Relative abundance of reworked specimens (%). d) *n*-hexacosan-1-ol index (%). Blue bars represent the timing of WMDW reinforcement periods and intensified upwelling conditions in the Alboran Sea. Pale grey bars represent the timing of WMDW weakening periods along with the steadier water column deduced in this study.

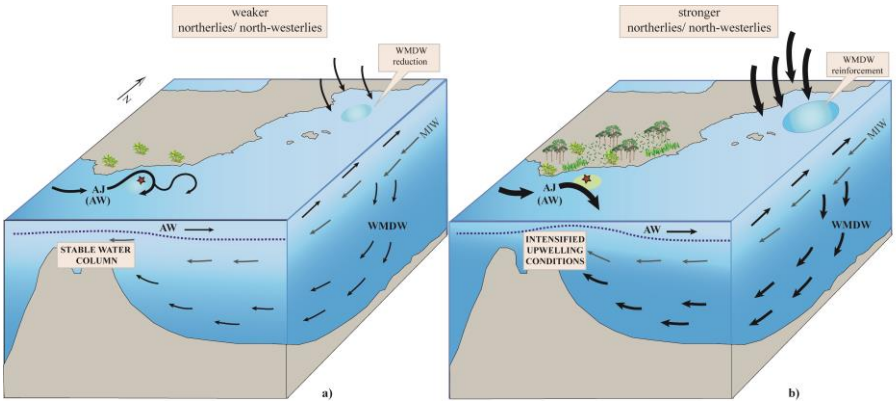

Figure 6. Proposed two-phase scenario: a) phase [1] and b) phase [2] as explained in the text. AW: Atlantic Water; AJ: Atlantic Jet; MIW: Intermediate Water; WMDW: Western Mediterranean Deep Water.

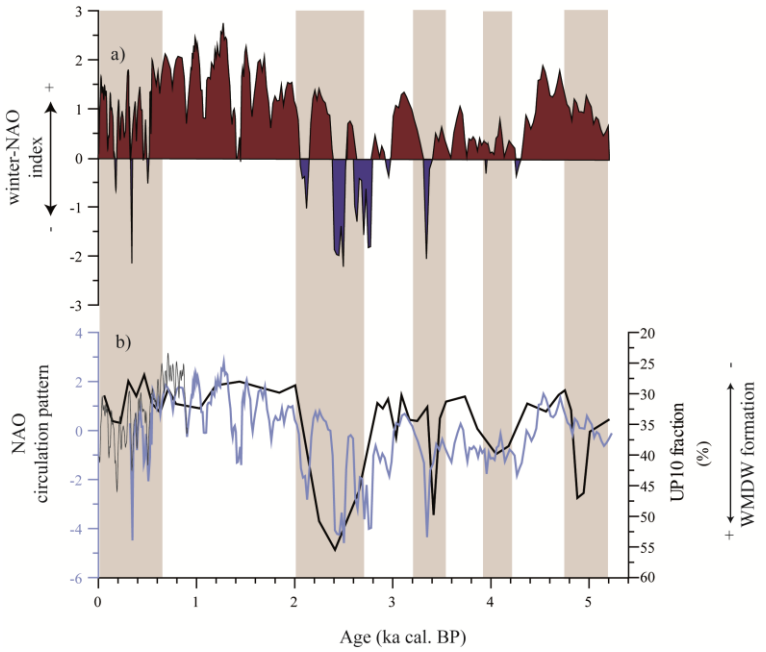

Figure 7. a) Winter-NAO index (Trouet et al., 2009; Olsen et al., 2012). Comparison of the winter-NAO circulation pattern according to Trouet et al. (2009), in brown, and to Olsen et al. (2012), in blue, with: b) the UP10 fraction (reversed vertical axis) from core MD95-2343 (Frigola et al., 2007). Pale brown bars represent the timing of periods of WMDW reinforcement and intensified upwelling conditions in the Alboran Sea.